Host−guest complexation-mediated codelivery of anticancer drug and photosensitizer for cancer photochemotherapy

A Submission to the Proceedings of the National Academy of Science USA

PHYSICAL SCIENCES: Chemistry

Guocan Yu,[a,1] Benyue Zhu,[b,1] Li Shao,[c,1] Jiong Zhou,[c,1] Manik Lal Saha,[d] Bingbing Shi,[d] Zibin Zhang,[b] Tao Hong,[b] Shijun Li,[b,2] Xiaoyuan Chen,[a,2] and Peter J. Stang[d,2]

[a]Laboratory of Molecular Imaging and Nanomedicine, National Institute of Biomedical Imaging and Bioengineering, National Institutes of Health, Bethesda, Maryland 20892, United States
[b]College of Material, Chemistry and Chemical Engineering, Hangzhou Normal University, Hangzhou 311121, P. R. China
[c]State Key Laboratory of Chemical Engineering, Center for Chemistry of High-Performance & Novel Materials, Department of Chemistry, Zhejiang University, Hangzhou 310027, P. R. China
[d]Department of Chemistry, University of Utah, 315 South 1400 East, Room 2020, Salt Lake City, Utah 84112, United States

[1]G.Y., B.Z., L.S. and J.Z. contributed equally to this work.

[2]To whom correspondence should be addressed. Email address: l_shijun@hznu.edu.cn; shawn.chen@nih.gov; stang@chem.utah.edu

Table of Contents (22 Pages)

Section A. Materials/General Methods/Instrumentation S2

Section B. Synthesis of Metallacage and Host−Guest Complexation S7

1. *Syntheses of **N_3-PEG-b-PLBG** and **M*** S7
2. *Host−guest complexation studies* S9

Section C. Preparation of MNPs and Theranostic Investigations S15

1. *Preparation of **MNPs*** S15
2. *In vitro and in vivo studies* S18

Section D. References S22

Section A. Materials/General Methods/Instrumentation

Azide-PEG-amine (N_3-PEG-NH_2, 2 kDa) was purchased from Biochempeg (Massachusetts, USA). Triphosgene, *L*-glutamic acid γ-benzyl ester and other reagents were purchased from Sigma-Aldrich and used as received. Solvents were either employed as purchased or dried according to procedures described in the literature. ^{1}H NMR and ^{31}P NMR spectra were recorded on a Bruker Avance III-300 or 400 spectrometer. ^{31}P{^{1}H} NMR chemical shifts are referenced to an external unlocked sample of 85% H_3PO_4. UV-vis spectra were taken on a Shimadzu UV-3150 spectrophotometer. Transmission electron microscopy (TEM) investigations were carried out on a Hitachi HT7700 instrument. The fluorescence experiments were conducted on a RF-5301 spectrofluorophotometer (Shimadzu Corporation, Japan). Dynamic light scattering (DLS) measurements were carried out using a 200 mW polarized laser source Nd:YAG (λ = 532 nm). The polarized scattered light was collected at 90 ° in a self-beating mode with a Hamamatsu R942/02 photomultiplier. The signals were sent to a Malvern 4700 submicrometer particle analyzer system. Molecular weights and distributions were determined by gel permeation chromatography (GPC) with a Waters 1515 pump and Waters 1515 differential refractive index detector (set at 30 ℃).

Preparation of the Metallacycle. Hexakis[4-(4′-pyridylethynyl)phenyl]benzene (**HPPB**), disodium terephthalate (**DSTP**), and ***c*Pt** in a 2:6:12 ratio were dissolved in the mixture of actone and water (*v*/*v* = 8:2). After stirring at 75 ℃ for 3 h, the solvent was removed by N_2 flow. Acetone (0.6 mL) was added, and the solution was stirred at 75 ℃ for an additional 5 h. The formed metallacage (**M**) was precipitated using diethyl ether.

Preparation of M⊃OEP-Loaded Nanoparticles (MNPs). The **MNPs** were fabricated through a matrix-encapsulation method. **N_3-PEG-*b*-PLBG** (50.0 mg) and **M⊃OEP** (30.0 mg) and were dissolved in 5 mL of acetone, then the solution was injected into MilliQ water (50 mL) under sonication. After sonication for 5 min, the organic solvent was completely removed *in vacuo*. Then, cRGDfK-DBCO (2.00 mg) was added into the solution, the mixture was further stirred for 8 h. Unloaded **M⊃OEP** and cRGDfK-DBCO in the solution was eleminated by passing through a PD-10 column. DLS and TEM were used to characterize these **MNPs**, and UV-vis spectroscopy was employed to confirm the actual loading amount of **M⊃OEP**. We assumed that no dissociation occurred for the host–guest complex during the preparation of nanoparticles. The method for the fabrication of the **M⊃OEP**-loaded nanoparticles without cRGDfK groups was similar to the preparation of **MNPs** without addition of cRGDfK-DBCO during the preparation process. The loading content was determined using the following formula:

Loading content (%) = [$m_{\mathbf{M}\text{-loaded}}$/($m_{\text{polymer}}$ + $m_{\mathbf{M}\text{-loaded}}$)]*100

Where the $m_{\mathbf{M}\text{-loaded}}$ and m_{polymer} are the masses of the encapsulated **M⊃OEP** in the **MNPs** and the diblock copolymer, respectively.

The method for the fabrication of **PNPs** was similar to the preparation of **MNPs**. Briefly, **N_3-PEG-*b*-PLBG** (50.0 mg) and **OEP** (10.0 mg) were solublized in 10 mL of acetone. The insolublized **OEP** was eliminated through centrifugation. The solution was injected into distilled water (50 mL), and the mixture was sonicated for 5 min. The organic solvent was completely removed *in vacuo*. Then, cRGDfK-DBCO (2.00 mg) was added into the solution, the mixture was further stirred for 8 h. Unloaded **OEP** and cRGDfK-DBCO in the solution was eleminated by passing through a PD-10 column. Notably, the loading content of **OEP** could be easily controlled by altering the ratio between the copolymers and **OEP**.

Release Studies. The release of ***c*Pt** and **OEP** from **MNPs** was determined through a dialysis strategy using ICP-MS and UV-vis spectroscopy. Briefly, **MNPs** were dissolved in phosphate buffered saline (PBS) to prepare a solution with the concentration of 3.00 mg/mL. The solution (2 mL) was transferred into a dialysis cassettes the molecular weight cut-off of 3.5 kDa and dialyzed against PBS (25 mL) at different pH in the absence/presence of guanosine triphosphate (0.10 mM). 100 μL of the solution was taken at pre-determined times from dialysate for measurement. At the same time, fresh PBS (100 μL) was added back into the dialysate. The released ***c*Pt** and **OEP** after different culture time was determined by ICP-MS and UV-vis spectroscopy, respectively.

Detection of $^1O_2$ Generation in Solution. In a typical experiment, **MNPs** were suspended in water containing 5.00 μM of singlet oxygen sensor green (SOSG) dye. The mixture was then placed in a cuvette and the solution was irradiated at 635 nm (0.5 W/cm^2) for different time, the fluorescence emission of SOSG (upon excitation at 470 nm) was measured using a fluorescence spectrophotometer. The generation of $^1O_2$ was also detected using anthracene-9,10-dipropionic acid disodium (ADPA) that could be bleached to its corresponding endoperoxide upon contact with $^1O_2$. A solution of ADPA in milli-Q water (1 mg/mL) was prepared containing **MNPs** (or **OEP**). The samples were irradiated with laser (635 nm, 0.5 W/cm^2) for different time. The reaction was monitored spectrophotometrically by recording the decrease of theabsorbance intensity at 378 nm.

Cell Culture. A2780 cell line was purchased from American Type Culture Collection (ATCC, Rockville MD), A2780CIS cell line was purchased from Sigma. A2780 and A2780CIS cells were cultured in RPMI-1640 medium containing FBS (10%) and penicillin/streptomycin (1%). A2780CIS cells were incubated in cisplatin-containing medium (2 μg/mL) for 10 days before experiments. Cells grew as a

monolayer and were detached upon confluence using trypsin (0.5% *w*/*v* in phosphate-buffered saline). The cells were harvested from cell culture medium by incubating in the trypsin solution for 5 min. The cells were centrifuged, and the supernatant was discarded. A 3.00 mL portion of serum-supplemented medium was added to neutralize any residual trypsin. The cells were resuspended in serum-supplemented medium at a concentration of 1.00×10^4 cells/mL. Cells were cultured at 37 ℃ and 5% CO_2.

Cytotoxicity Evaluation. The cytotoxicity against the cell lines was evaluated by a 3-(4′,5′-dimethylthiazol-2′-yl)-2,5-diphenyl tetrazolium bromide (MTT) assay. The cells were seeded at a density of 1.00×10^4 cells/well, and cultured for 12 h for attachment. Then the cells were cultured with fresh serum-supplemented medium without/with cisplatin, ***c*Pt**, **PNPs**, and **MNPs** at various concentrations for 24 h. For the groups treated with **PNPs** + L (mono-PDT) and **MNPs** + L (photochemotherapy), the cells were irradiated with light at 635 nm (0.2 W/cm^2, 5 min) after 12 h incubation. After irradiation, the cells were further incubated for 12 h. Then MTT solution (20 μL, 5.00 mg/mL) was added to each well. After incubating the cells at 37 ℃ for 4 h, the MTT solution was removed and the cells were washed three times by PBS. DMSO (100 μL) was added to dissolve the insoluble formazan crystals, and the absorbance was measured by a spectrophotometer (570 nm). The cells without any treatment were utilized as a control. All experiments were carried out with five replicates.

Intracellular $^1O_2$ Detection. The generation of $^1O_2$ inside cells was detected immediately after the photosensitization experiments by using a singlet oxygen indictor. Briefly, the cells were cultured with **MNPs** for 12 h. DCF-DA (5.00 μM) was added and the cells were incubated for another 4 h. The cells pre-treated with vitamin C were used as a control, in which vitamin C (50.0 μM) and DCF-DA were added into the medium together. Then the cells were subjected to photosensitization by using 635 nm laser irradiation with the density of 0.2 W/cm^2 for 5 min. After irradiation, the medium was removed carefully and the cells were washed with PBS three times. The cells were fixed and the nucleus were stained with DAPI. The images were taken using a LSM-510 confocal laser scanning microscope (CLSM, ZEISS LSM780). Additionally, flow cytometry was also used to monitor the formation of DCF by monitoring the intracellular green fluorescence.

Platinum Efflux Determination. In order to understand the cellular efflux of the platinum-based drugs, we determined the efflux percent of cisplatin and ***c*Pt**. A2780 and A2780CIS cells were incubated with cisplatin or **MNPs** with the platinum concentration of 1 μM for 8 h, and the culture medium was replaced by fresh medium and further incubated for 1, 4, and 8 h. The platinum amount detected in the culture medium were compared with the uptake amounts to give the efflux percent.

***In Vitro* Cellular Internalization of MNPs Determined by CLSM and ICP-MS**. A2780CIS cells were incubated with **MNPs** at 37 ℃ for 8 h, then the cells were washed three times with PBS and fixed with fresh 4.0% formaldehyde at room temperature for 15 min. After washing with PBS, the cells were stained with 4′,6-diamidino-2-phenylindole (DAPI) or fluorescein isothiocyanate-labeled phalloidin (FITC) (1 μg/mL) for 15 min. The images were taken using a LSM-510 confocal laser scanning microscope (CLSM, ZEISS LSM780). The cullular internalization of **MNPs** was also monitored using ICP-MS. A2780CIS cells were seeded at a density of 2.00×10^5 cells/well in 12-well cell culture plates. The cells were left to grow for 24 h in media containing 10% FBS at 37 ℃ and 5% CO_2 atmosphere. After 24 h, **MNPs** and the NPs without cRGDfk (the concentration of Pt was kept at 10 μM) were added into the wells and the cells were incubated for 1 h, 2 h, and 4 h, respectively. Following incubation, the cells were washed, digested and collected, and the intracellular Pt amount was determined by ICP-MS. To confirm internalization *via* receptor-mediated endocytosis, a competition assay was performed by pre-treating the cells with free cRGDfK for 30 min. All experiments were carried out with three replicates.

Flow Cytometry for Apoptosis Assay. A2780CIS cells were seeded in 6-well plates at a density of 3×10^5 cells/well and incubated in culture medium for 24 h at 37 ℃. After that, the culture medium containing cisplatin, ***c*Pt**, **PNPs**, or **MNPs** was added. For chemotherapy, the cells were cultured for 24 h. For PDT, the cells were cultured for 12 h followed by laser irradation (635 nm, 0.2 W/cm^2) for 5 min. Then the cells were further cultured for 12 h. After that, the cells were thoroughly washed with PBS and harvested with typsin. The collected cells were washed three times with PBS and resuspended in 0.3 mL of PBS. The cells were stained with Annexin V-FITC and propidium iodide according to the protocal. The cells were incubated for 15 min at room temperature in the dark and added with 400 μL of 1× binding buffer. The stained cells were analyzed by flow cytometry. A total of 1×10^4 events were counted for analysis. It should be noted that **PNPs** without laser irradiation were utilized as a control to eliminate the influence of **OEP** fluorescence.

Tumor Model. Nude mice (4 weeks old, ~20 g body weight) were purchased from Zhejiang Academy of Medical Sciences and maintained in a pathogen-free environment under controlled temperature (24 ℃). Study protocols involving animals were approved by the Zhejiang University Animal Care and Use Committee. The nude mice were injected subcutaneously in the right flank region with 200 μL of cell suspension containing 5×10^6 A2780CIS cells. The tumors were allowed to grow to ~100 mm^3 before anti-tumor studies. The tumor volume was calculated as (tumor length) × (tumor width)^2/2.

Pharmacokinetics and Tissue Distributions. Mice received cisplatin (1.00 mg Pt/kg) or **MNPs** (1.00 mg Pt/kg) by tail vein injection (n = 4). Blood was collected by cardiac puncture and kept in heparinized

tubes. The amount of platinum in the plasma was determined by ICP-MS. The skin, muscle, intestine, heart, lung, liver, kidney, spleen, stomach, bone, and tumor were excised at different time post *i.v.* injection and kept in dry ice before analysis. Organs were digested in concentrated nitric acid. The amount of platinum was analyzed by ICP-MS.

***In Vivo* Antitumor Activity.** Tumor volume and body weights were measured for individual animals in all experiments. The mice were divided into six treatment groups randomly (n = 8), when the mean tumor volume reached about 100 mm^3 and this day was set as day 0. The mice were administered intravenously with PBS, laser, cisplatin (1.00 mg Pt/kg), M**NPs** (1.00 mg Pt/kg), P**NPs** + L (**OEP** concentration was same as that in M**NPs**), and M**NPs** + L. For chemotherapy (cisplatin and M**NPs**), the formulations were injected every 3 days for three times. For photodynamic therapy and photochemotherapy, the mice only received one laser irradiation (635 nm, 0.2 W/cm^2, 15 min) at 24 h post the first injection. Tumor volume and body weight were measured every 3 days.

Tissue Histopathology Evaluation. In the histological assay, the heart, liver, spleen, lung, kidney, and tumor tissues were fixed in 4% paraformaldehyde for 24 h. The specimens were dehydrated in graded ethanol, embedded in paraffin, and cut into 5 mm thick sections. The fixed sections were deparaffinized and hydrated according to a standard protocol and stained with hematoxylin and eosin (H&E) for microscopic observation. Apoptosis of the tumor cells in the mice after treatments was determined by the TUNEL method according to the manufacturer's instructions.

Statistical Analysis. Data are expressed as mean standard deviation (SD). Analysis of variance (ANOVA), followed by Student's *t*-test, was used to determine the significant differences among the groups (**$P < 0.01$, and ***$P < 0.001$).

Section B. Synthesis of Metallacage and Host−Guest Complexation

1. Syntheses of ***N_3-PEG-b-PLBG*** *and* ***M***

Synthesis of N_3-PEG-*b*-PLBG. $_L$-Glutamic acid γ-benzyl ester (2.37 g, 10.0 mmol) and triphosgene (2.7 g, 3.9 mmol) were suspended in 100 mL ethyl acetate, and the mixture was stirred under reflux for 3 h until the solution became clear. The crude product was extracted with 100 mL cold nanopure water, 100 mL cold saturated sodium bicarbonate solution, and 100 mL cold saturated sodium chloride solution. The organic layer was dried over $MgSO_4$, concentrated to remove ethyl acetate. White powder was obtained after twice precipitation from ethyl acetate into hexane and dried. The obtained powder and the macromolecular initiator N_3-PEG-NH_2 were dissolved in anhydrous DMF. Continuous nitrogen flow was used to promote polymerization at room temperature. ^{1}H NMR was used to monitor the polymerization, ~99% monomer was consumed within 48 h. The polymer was purified by precipitation from DMF into diethyl ether under vigorous stirring. The solid was washed with diethyl ether to afford a white powder after drying in vacuum at room temperature. The molecular weight and composition of **N_3-PEG-*b*-PLBG** were determined by GPC and ^{1}H NMR studies. From ^{1}H NMR spectrum (Figure S1), the polymerization degree of PLBG segment was calculated to be 68. From GPC curve (Figure S2), the molecular weight of **N_3-PEG-*b*-PLBG** was measured to be 19.1 kDa with a PDI value of 1.16.

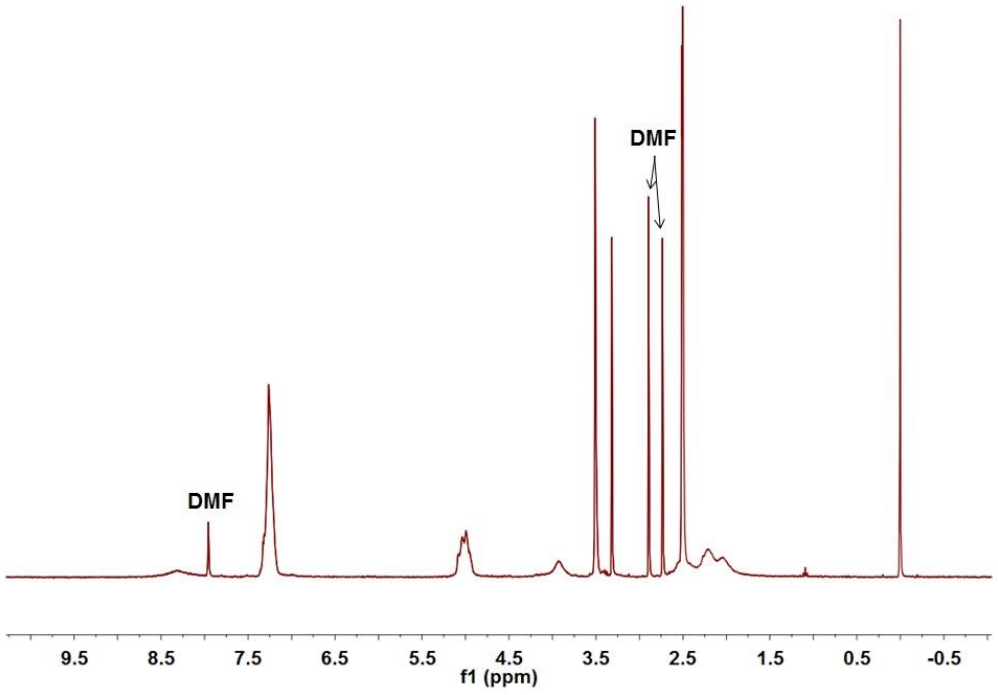

Figure S1. ^{1}H NMR spectrum (300 MHz, DMSO-d_6, room temperature) of **N_3-PEG-PLBG**.

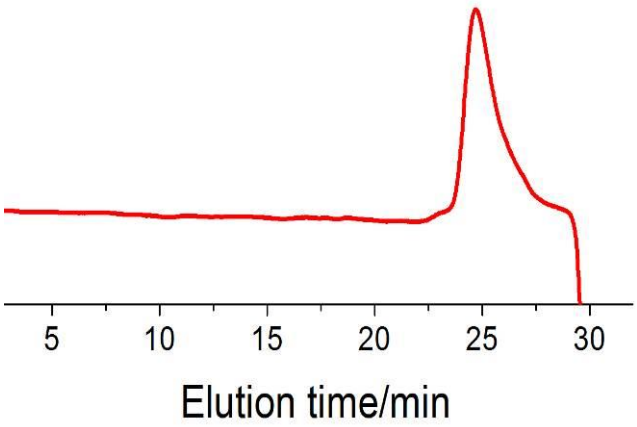

Figure S2. GPC curve of **N_3-PEG-PLBG**.

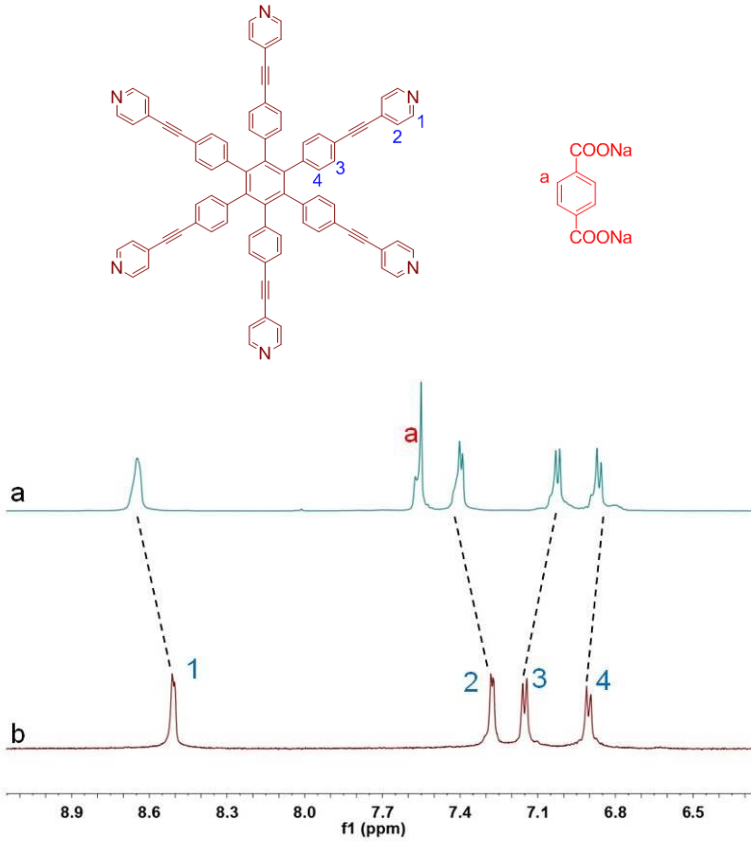

Figure S3. ^{1}H NMR spectra (CD_2Cl_2/CD_3CN = 1/1, 298 K) of (a) **M** and (b) **HPPB**.

2. Host−guest complexation studies

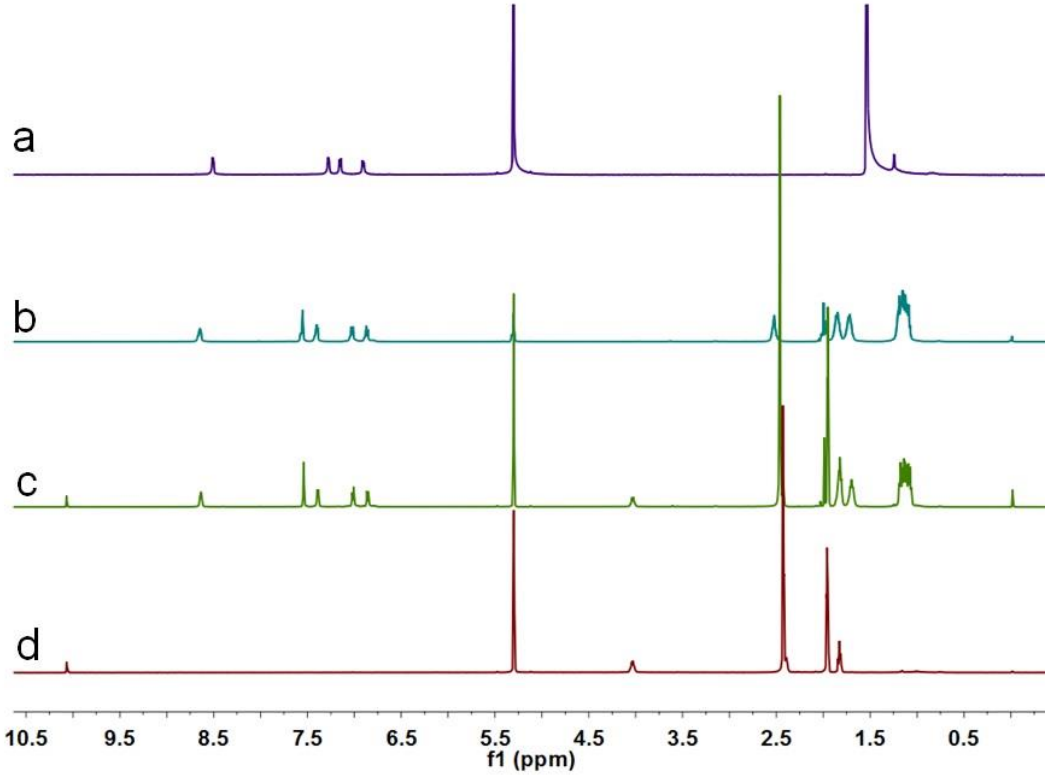

Figure S4. ^{1}H NMR spectra (CD_2Cl_2/CD_3CN = 1/1, 298 K) of (a) **HPPB**, (b) **M**, (c) **M⊃OEP**, and (d) **OEP**.

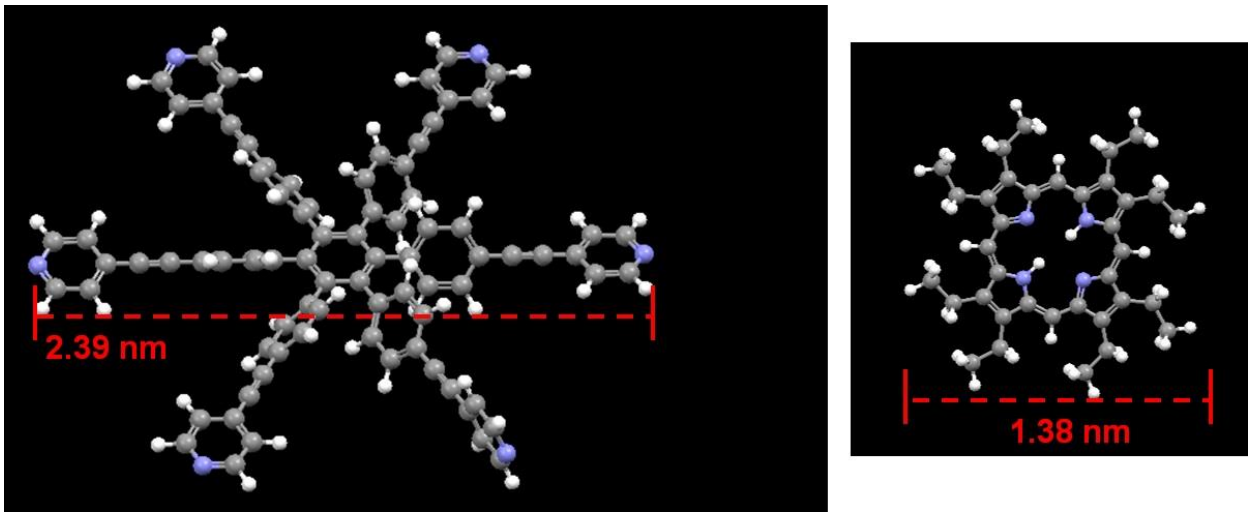

Figure S5. The energy-minimized structures of **HPPB** and **OEP** calculated using ChemBio3D.

From molecular modeling, we knew that the size of the resultant metallacage was large enough to encapsulate the photosensitizer guest (**OEP**).

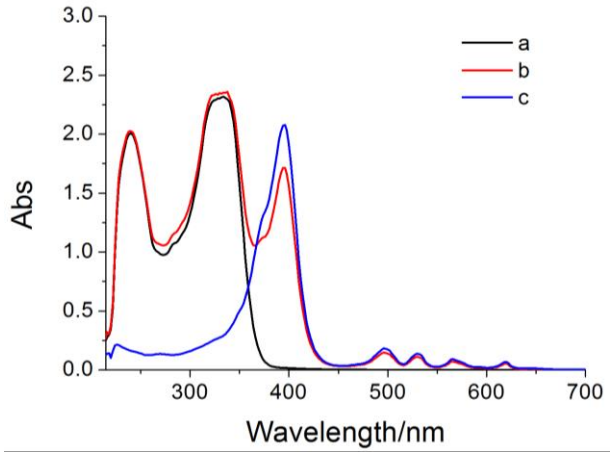

Figure S6. UV-vis spectra of (a) **M**, (b) **M⊃OEP**, and (c) **OEP**.

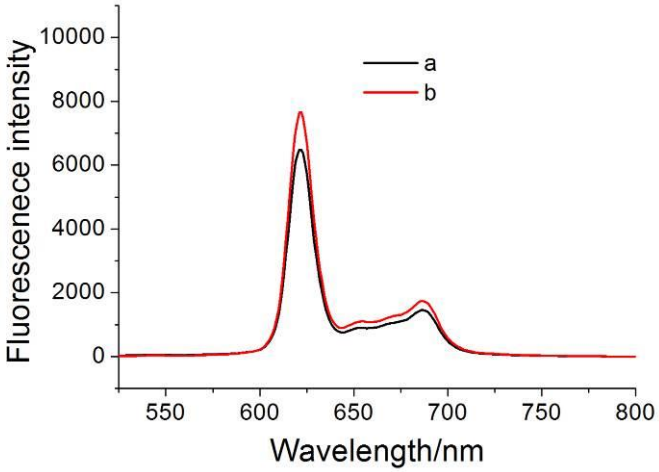

Figure S7. Fluorescence spectra of of the solution containing (a) **M⊃OEP** and (b) **OEP**.

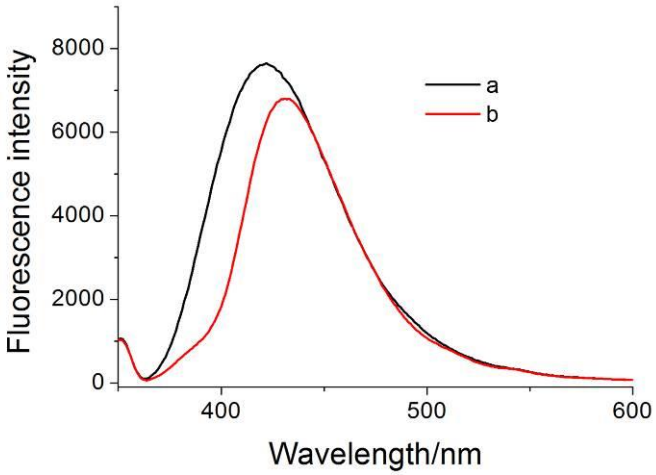

Figure S8. Fluorescence spectra of the solution containing (a) **M** and (b) **M⊃OEP**.

To determine the stoichiometry and association constant between the host and the guests, ^{1}H NMR titrations were carried out with solutions that had a constant concentration of **OEP** and varying concentrations of **M**. By a non-linear curve-fitting method, the association constant (K_a) of **M⊃OEP** was estimated. By a mole ratio plot, 1:1 stoichiometry was obtained.

The non-linear curve-fitting was based on the equation:[S1]

$$\Delta\delta = (\Delta\delta_\infty/[G]_0)\ (0.5[H]_0 + 0.5([G]_0+1/K_a)-(0.5\ ([H]_0^2+(2[H]_0(1/K_a - [G]_0)) + (1/K_a + [G]_0)^2)^{0.5})) \quad \text{(Eq. S1)}$$

Where $\Delta\delta$ is the chemical shift change of H_α on **OEP** at $[G]_0$, $\Delta\delta_\infty$ is the chemical shift change of H_α when the guest is completely complexed, $[G]_0$ is the fixed initial concentration of the host, and $[H]_0$ is the initial concentration of **M**.

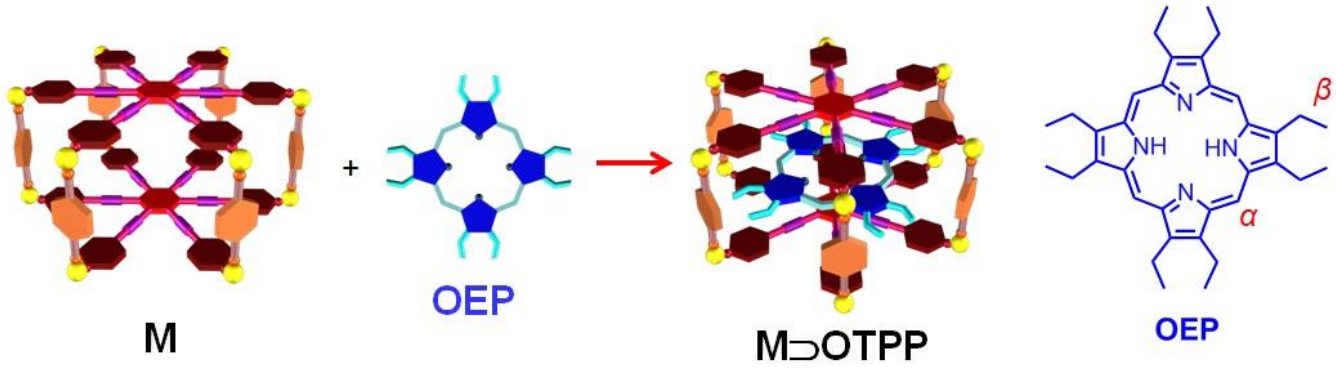

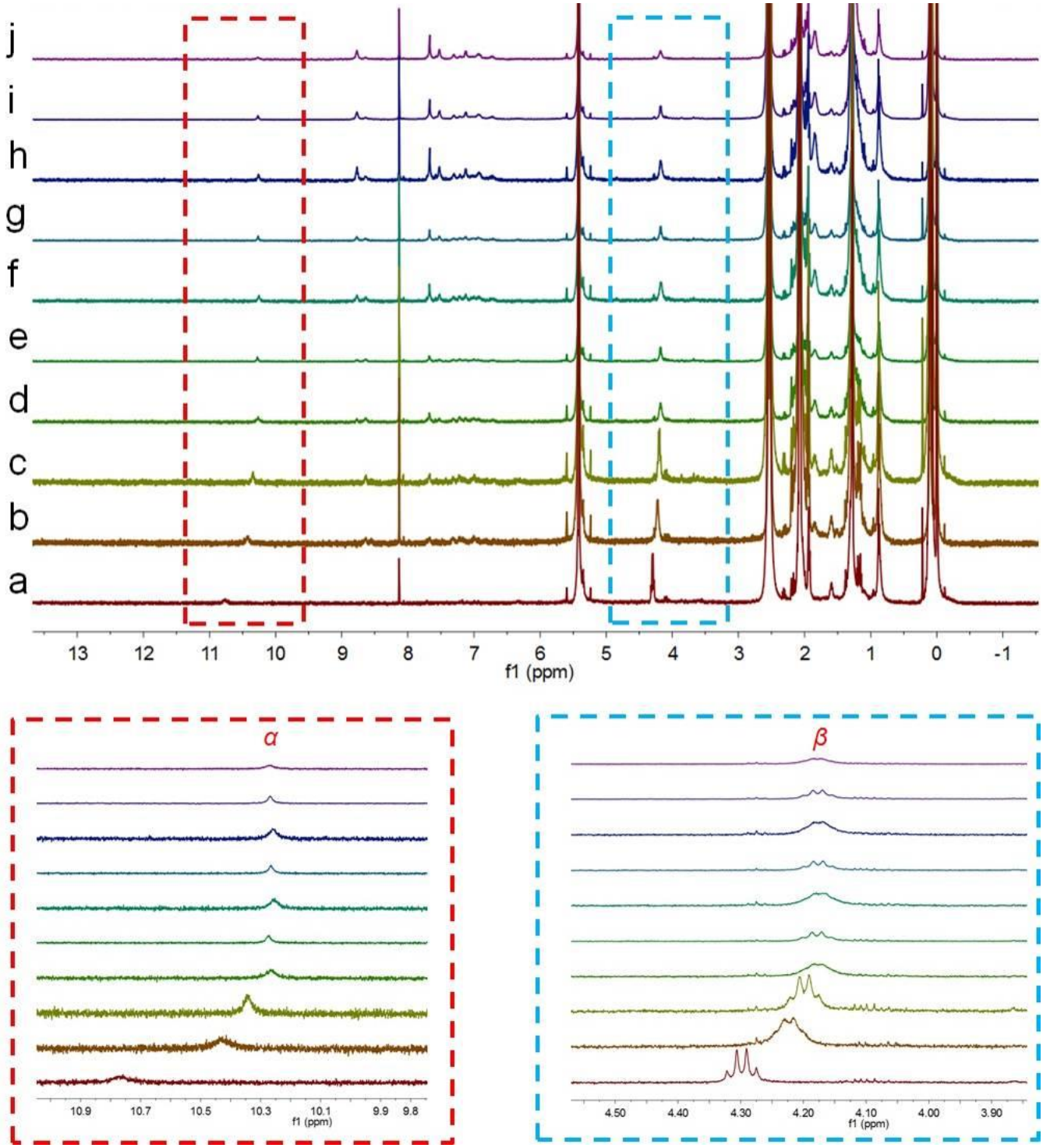

Figure S9. Partial ^{1}H NMR spectra (400 MHz, CD_2Cl_2/CD_3CN = 1/1, 298 K) of **OEP** at a concentration of 0.10 mM upon addition of **M**: (a) 0.00 mM, (b) 0.039 mM, (c) 0.058 mM, (d) 0.077 mM, (e) 0.095 mM, (f) 0.148 mM, (g) 0.182 mM, (h) 0.246 mM, (i) 0.412 mM, and (j) 0.507 mM.

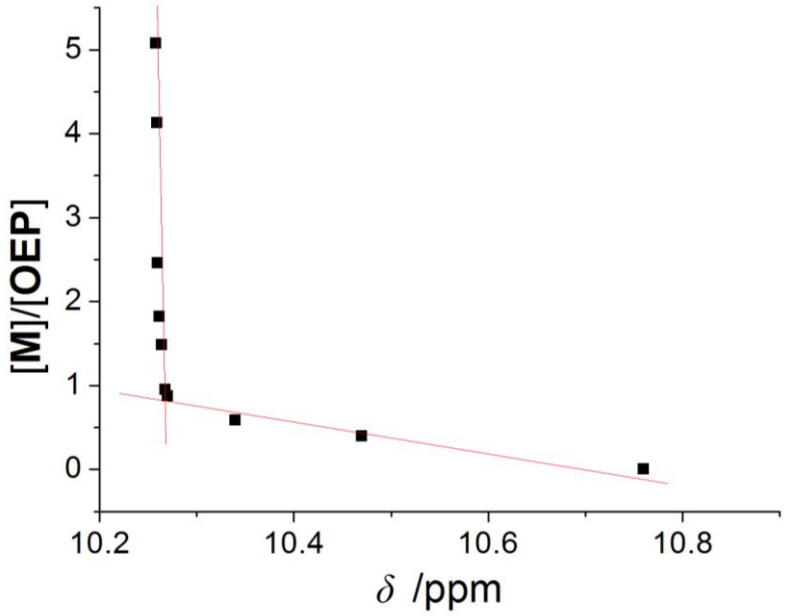

Figure S10. Mole ratio plot for **M** and **OEP**, indicating a 1:1 stoichiometry.

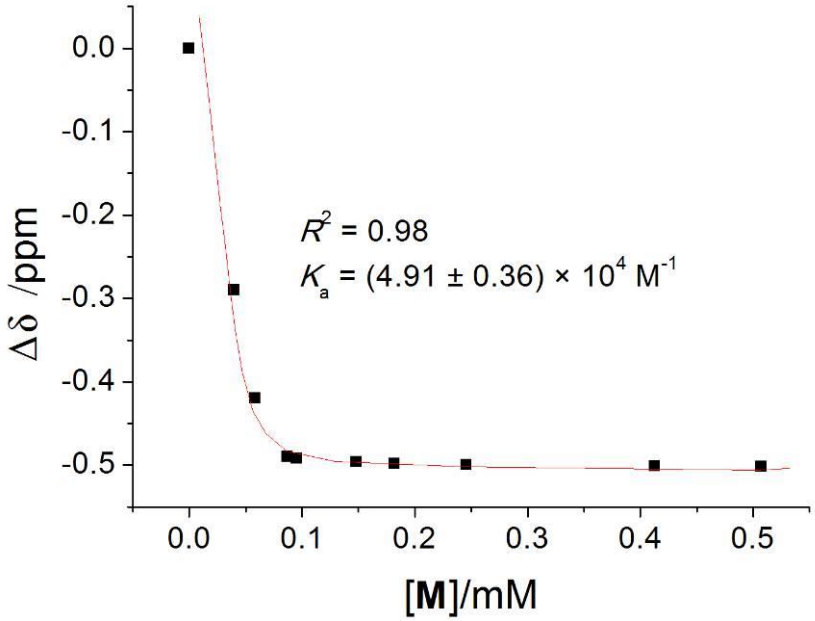

Figure S11. The chemical shift changes of H_α on **OEP** upon addition of **M**. The red solid line was obtained from the non-linear curve-fitting using Eq. S1.

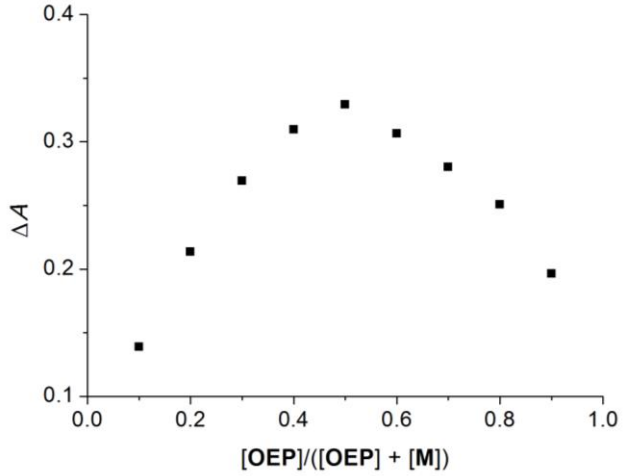

Figure S12. Job's plot for the solutions of **M** and **OEP** ([**M**] + [**OEP**] = 50 μM).

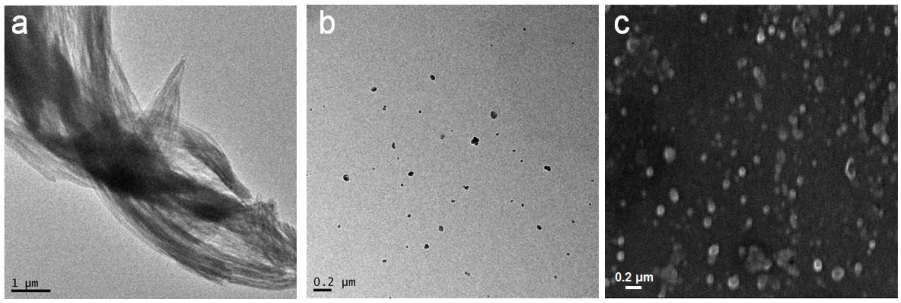

Figure S13. TEM image of the self-assemblies formed from (a) **OEP** and (b) **M⊃OEP**, in water. (c) SEM image of the self-assemblies formed from **M⊃OEP**.

Section C. Preparation of MNPs and Theranostic Investigations

*1. Preparation of **MNPs***

Table S1. Loading capability and stability evaluations.

Polymer (mg)	**OEP** (mg)	LE (%)[a]	LC (%)[b]	Stability	Polymer (mg)	**M⊃OEP (mg)**	LE (%)[a]	LC (%)[b]	Stability
100	20	43.7	8.04	No precipitation within 1 d	100	20	93.5	15.8	No precipitation within 1 d
100	40	37.8	13.1	Partial precipitation within 8h	100	40	89.3	26.4	No precipitation within 1 d
100	60	28.9	14.8	Partial precipitation within 8h	100	60	73.4	30.6	No precipitation within 1 d
100	80	21.6	14.7	Partial precipitation within 8 h	100	80	60.2	32.5	Partial precipitation within 8 h

[a] Loading efficiency (LE) = M_{load}/M_{add} * 100%, where M_{add} and M_{load} represent the mass added during the preparation of NPs and loaded by the NPs, respectively.

[b] Loading content (LC) = $M_{load}/(M_{load} + M)$ * 100%, where M represents the polymer mass used during the preparation of NPs.

[c] The size of the NPs was measured by DLS.

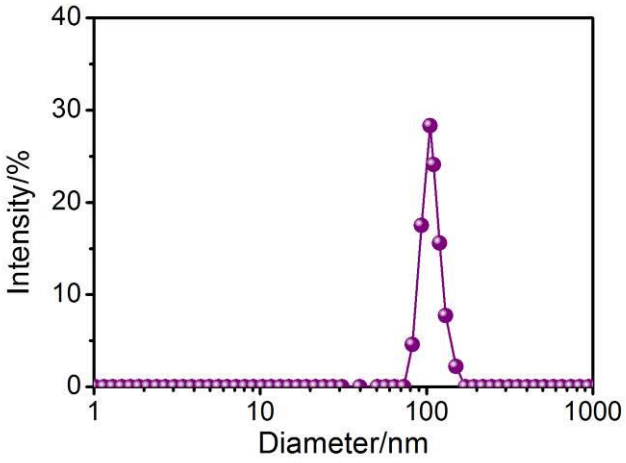

Figure S14. DLS result of NPs self-assembled from **M⊃OEP** and **N_3-PEG-PLBG** without cRGDfK. The average diameter was 104 ± 6.9 nm.

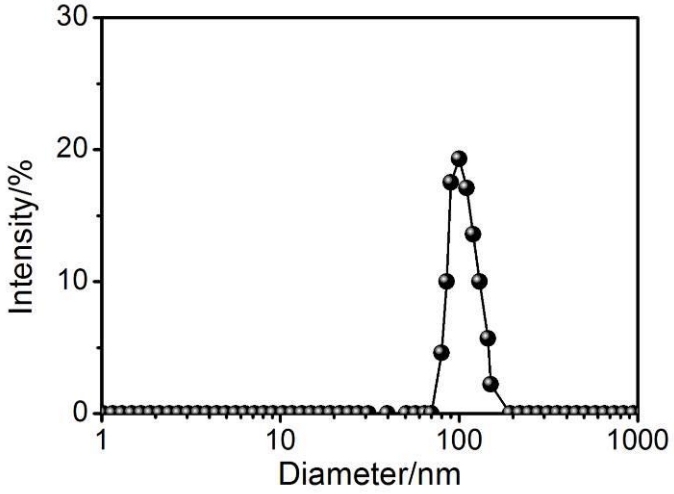

Figure S15. DLS result of **MNPs**. The average diameter was 109 ± 8.4 nm.

Compared with Fig. S14 and S15, negligible changes in diameter of the nanoparticles were detected before and after conjugation of a targeting ligand through a copper-free click reaction, demonstrating the *in situ* post-modification did not changes the size of the nanoparticles.

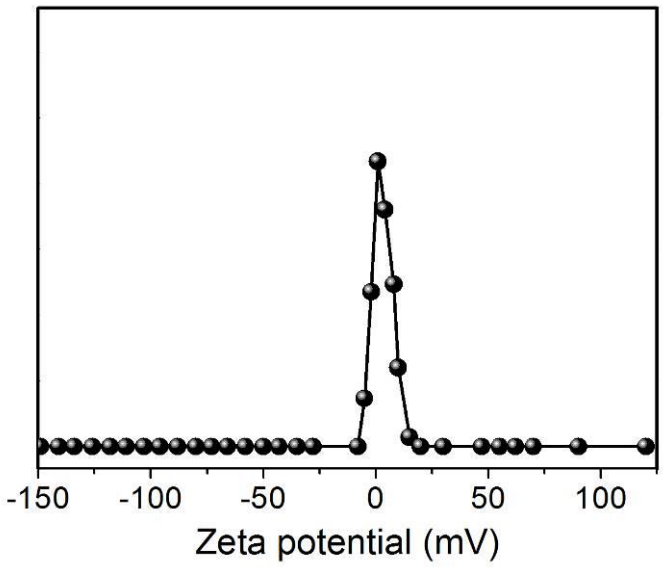

Figure S16. Zeta potential of **MNPs** in PBS.

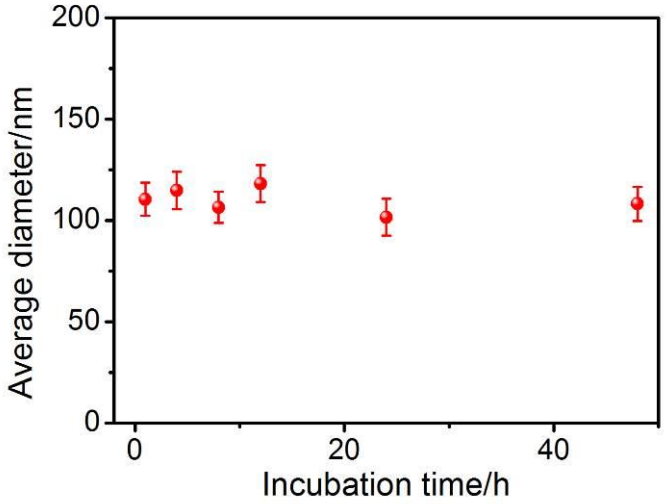

Figure S17. Average diameter changes of **MNPs** determined by DLS in PBS containing FBS (10%).

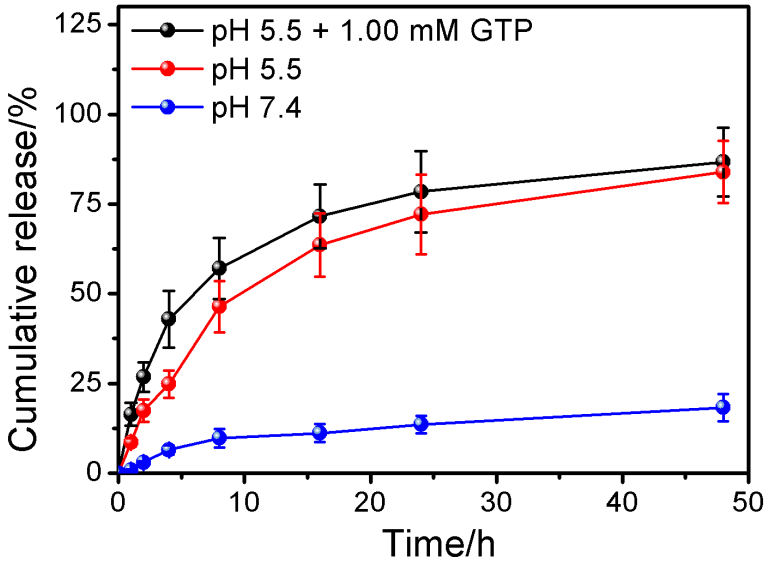

Figure S18. Release behaviors of **OEP** under different conditions.

2. In vitro and in vivo studies

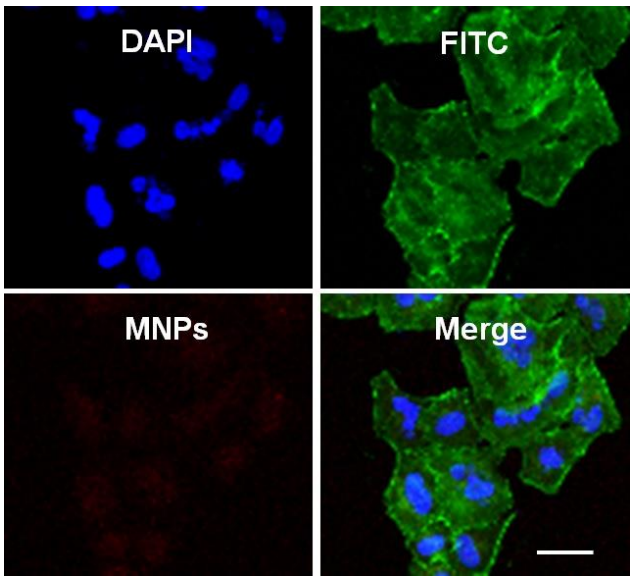

Figure S19. CLSM images of A2780CIS cells after incubation with **MNPs** for 8 h pre-treated with free cRGDfK for 30 min. The nucleus were stained with DAPI and the β-actin was stained with FITC.

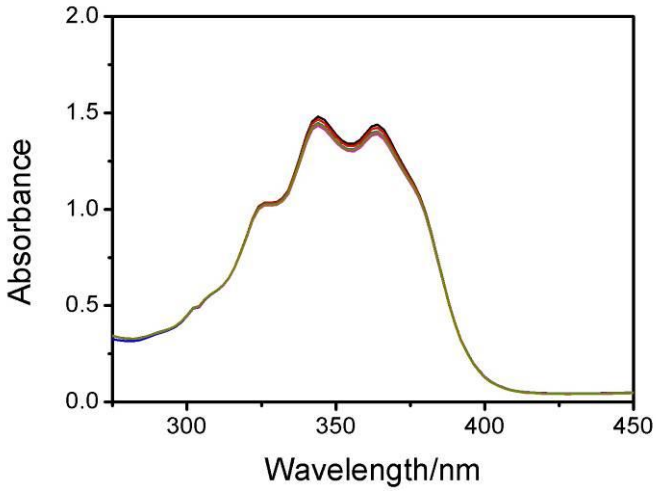

Figure S20. UV-vis spectra of APDA in the presence of **OEP** upon laser irradiation for different time.

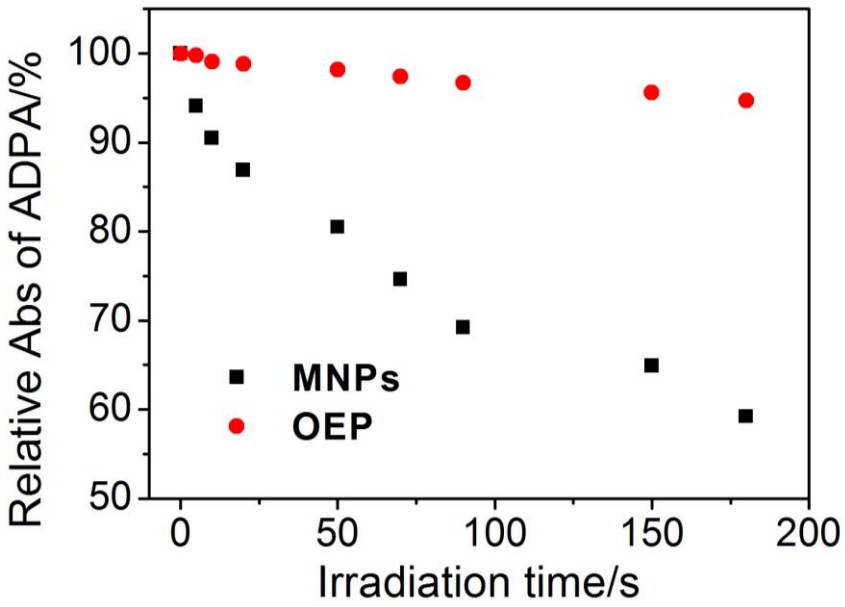

Figure S21. Relative absorbance changes of APDA at 378 nm in the solution containing **MNPs** or **OEP** upon different irradiation time.

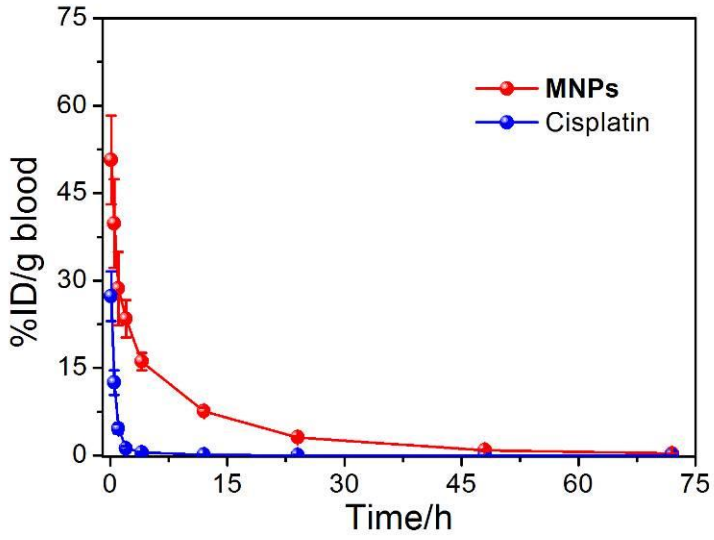

Figure S22. *In vivo* pharmacokinetics of cisplatin and **MNPs** analysed by ICP-MS.

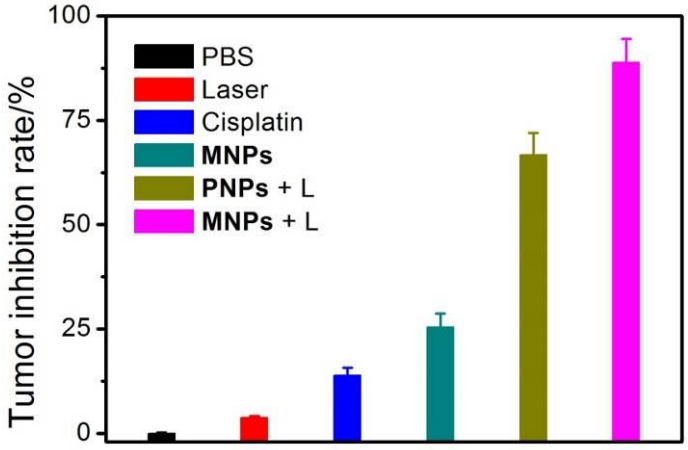

Figure S23. Tumor inhibition rate of the mice administrated with different formulations.

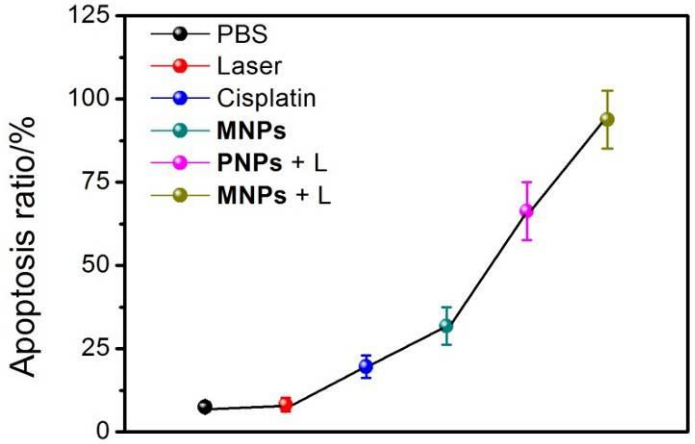

Figure S24. Apoptosis ratio in the tumor site of the mice treated with different formulations.

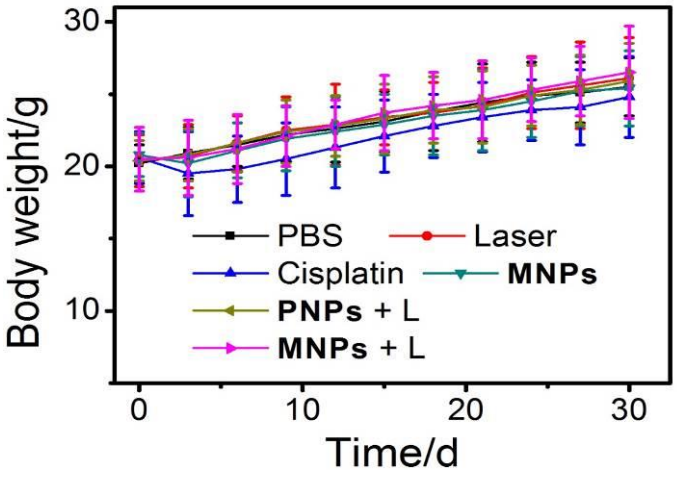

Figure S25. Body weight changes of the A2780CIS tumor-bearing mice treated with different formulations.

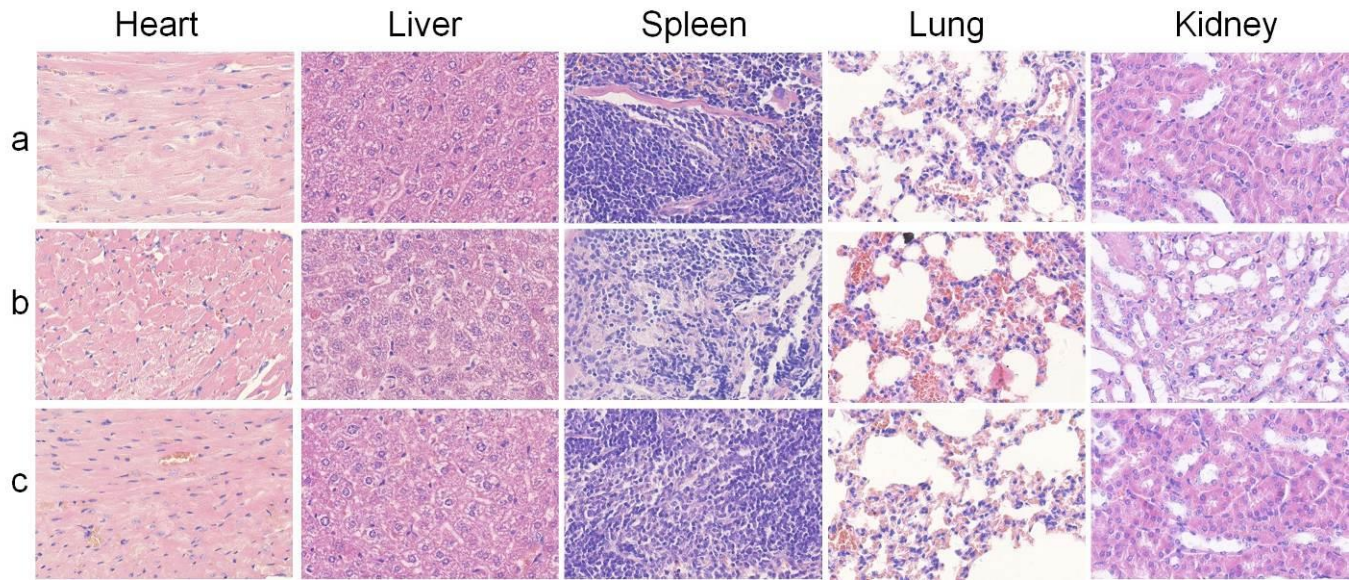

Figure S26. H&E stained images of heart, liver, spleen, lung and kidney from different groups treated with (a) PBS, (b) cisplatin, and (c) **MNPs** + L.

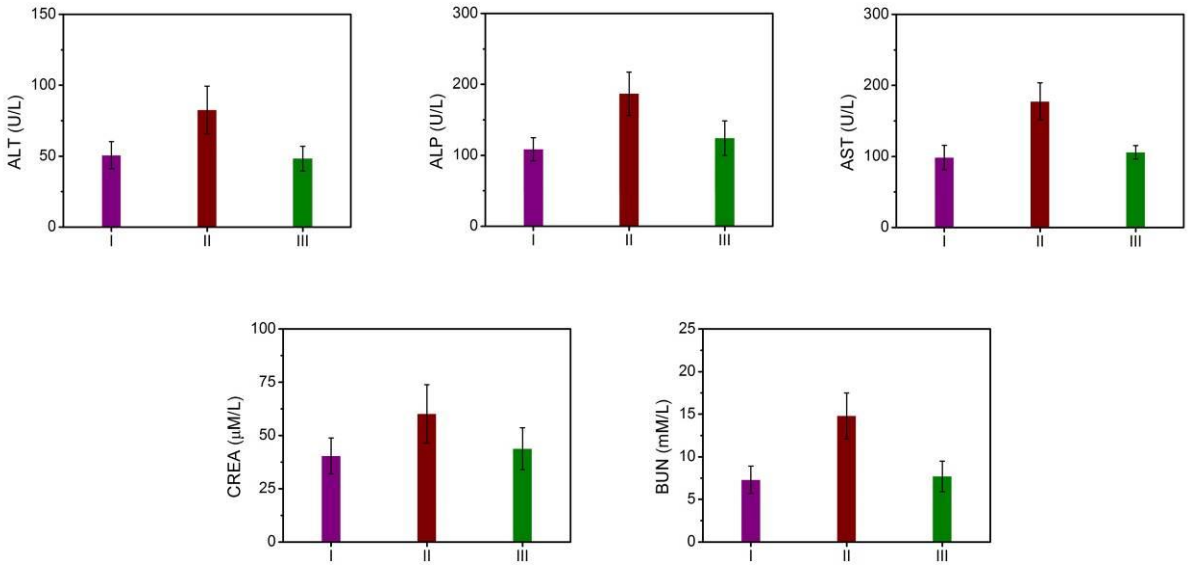

Figure S27. The variations of aspartate aminotransferase (AST), alanine aminotransferase (ALT), alkaline phosphatase (ALP), creatinine (CREA) and blood urea nitrogen (BUN) of the mice after treatment with (I) PBS, (II) cisplatin, and (III) **MNPs** + L at 12 d post-injection. Data are expressed as mean ± s.d. of three independent experiments.

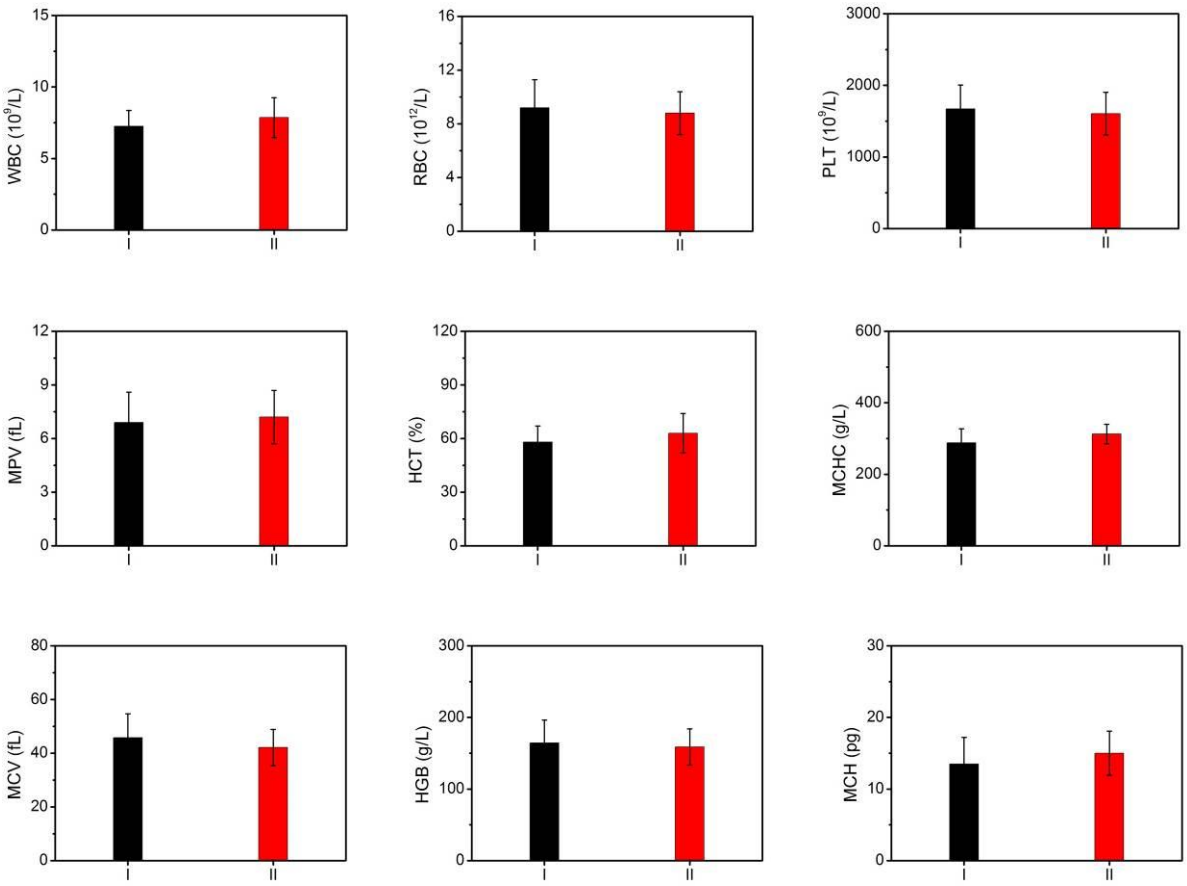

Figure S28. The variations of white blood cells (WBC), red blood cells (RBC), platelets (PLT), mean platelet volume (MPV), mean corpuscular volume (MCV), mean corpuscular hemoglobin concentration (MCHC), mean corpuscular hemoglobin (MCH), hematocrit (HCT), and hemoglobin (HGB) of the mice after treatment with (I) PBS, and (II) **MNPs** + L at 12 d post-injection. Data are expressed as mean ± s.d. of three independent experiments.

Section D. References

S1 (a) Ashton PR, et al. (1996) Self-assembly, spectroscopic, and electrochemical properties of [*n*]rotaxanes. *J Am Chem Soc* 118(21):4931−4951; (b) Inoue Y, et al. (1998) Inclusion complexation of (cyclo)alkanes and (cyclo)alkanols with 6-*O*-modified cyclodextrins. *J Chem Soc Perkin Trans* 2:1807−1816.